TM mode analysis in a metamaterial based dielectric waveguide

Jin, Cheng; Alphones, Arokiaswami; Dhirendra, M. M.

2012

Jin, C., Alphones, A., & Dhirendra, M. M. (2013). TM mode analysis in a metamaterial based dielectric waveguide. Progress In Electromagnetics Research M, 24, 221-234.

https://hdl.handle.net/10356/98479

https://doi.org/10.2528/PIERM12042407

Progress In Electromagnetics Research M, Vol. 24, 221–234, 2012

TM MODE ANALYSIS IN A METAMATERIAL BASED DIELECTRIC WAVEGUIDE

C. Jin*, A. Alphones, and M. M. Dhirendra

School of Electrical and Electronic Engineering, Nanyang Technological University, Singapore 639798, Singapore

Abstract—A TM mode analysis in a metamaterial based dielectric waveguide is proposed and introduced. Rigorously derived from Maxwell's equations, the dispersion properties are focussed on the fundamental properties of bound, surface and leaky modes of metamaterial based dielectric waveguide. Comparing with the conventional right handed material based waveguide, typical backward wave characteristic of volume and surface wave modes are found from the distribution of Poynting power to the transverse direction of waveguide.

1. INTRODUCTION

Metamaterial with simultaneous negative permittivity ($\varepsilon = \varepsilon_r\varepsilon_0$) and permeability ($\mu = \mu_r\mu_0$) was first investigated theoretically by Veselago in 1968 [1]. After two decades, negative permittivity materials [2], negative permeability ring resonators [3] and composite medium [4, 5] were practically realized to demonstrate the concept of left-handedness. Later, composite right/left handed transmission lines (CRLH TLs) were proposed to design low-loss and broadband metamaterials [6, 7]. In 2009, a novel structure named as double periodic composite right/left handed transmission line (DP-CRLH TL) was proposed [8–11]. Compact devices for communication system applications, like small leaky-wave antennas (LWAs) [12–15] and compact filters [16–18] are realized based on CRLH TLs.

Similar to right-handed materials ($\varepsilon > 0$ and $\mu > 0$) [19–22], the analysis for the composite right/left handed (CRLH) materials is aimed at determining the propagation constant γ (phase constant β and attenuation constant α) and dispersion characteristics, especially

Received 24 April 2012, Accepted 27 May 2012, Scheduled 4 June 2012

* Corresponding author: Cheng Jin (jincheng@ieee.org).

for the left-handed (LH) region ($\varepsilon < 0$ and $\mu < 0$) and stopband region ($\varepsilon\mu < 0$). Investigation on the CRLH materials based on the transmission line theory, Floquet Theorem [6, 7] and equivalent circuit theory [23] have been proposed based on static methods or quasi-static methods. The transmission line characteristics are calculated from the electrostatic properties of the structure and the nature of the mode of propagation is considered to be TEM mode. For structures like microstrip lines, waveguide and 3-D materials, it is not capable of supporting a pure TEM mode, and the static methods cannot fully describe these hybrid modes. Small longitudinal components of both the electric and magnetic fields need to be present to satisfy boundary conditions. These modes, in a lossless CRLH guiding structures, not only represent waves that propagate without attenuation ($\beta \neq 0$ and $\alpha = 0$) and decay exponentially without phase variation ($\beta = 0$ and $\alpha \neq 0$), but also complex wave, leaky-wave, surface wave and lossy surface wave, etc.

For simplicity and without loss of generality, the transverse magnetic (TM) mode is considered for basic uniform rectangular waveguide analysis as shown in Figure 1. The grounded rectangular waveguide is assumed to be filled with pure right-handed material, pure LH material, material with $\varepsilon\mu < 0$ or CRLH material. The dispersion properties are rigorously derived from Maxwell's equation and give a considerable physical insight into the overall behavior of the structure [21, 24]. For different cases, the wave will propagate in different modes: forward/back-fire leaky wave mode, forward/back-fire surface wave mode, decaying radiate mode and lossy surface wave.

For simplicity and without loss of generality, the transverse

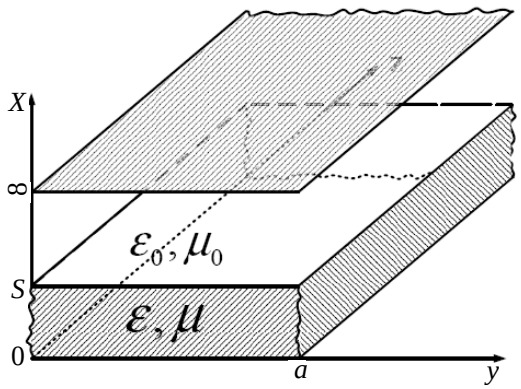

Figure 1. Geometry of the basic uniform rectangular waveguide.

magnetic (TM) mode is considered for basic uniform rectangular waveguide analysis as shown in Figure 1 in this paper. The dispersion analysis is used without invoking any static approximations to determine the propagation constant while estimating constitutive equation of permeability and permittivity media [21, 24]. The dispersion properties are rigorously derived from Maxwell's equation and give a considerable physical insight into the overall behavior of the structure. Pure right-handed material, pure LH material, material with $\varepsilon\mu < 0$ and CRLH material are discussed for the grounded dielectric waveguide. For different cases, the wave will propagate in different modes: forward/back-fire leaky wave mode, forward/back-fire surface wave mode, decaying radiate mode and lossy surface wave. Some of modes do not contribute directly to the aperture field. However, they mite contribute towards end-fire leaky-wave radiation.

2. FORMULATION OF THE DISPERSION RELATION

The geometry of the problem analyzed is shown in Figure 1. The lossless dielectric film (ε, μ) occupies the region $0 < x < s$ and is covered by the free space (ε_0, μ_0). For the sake of simplicity and without loss of generality, only TM mode with nonvanishing field components H_y, E_x and E_z have been considered to be propagating in xz-plane. The wave is assumed to be uniform in the y-direction ($\partial/\partial y = 0$) and have the time dependence $\exp(j\omega t)$ [21]. From Maxwell's equations, the magnetic field H_y in the waveguide satisfies the Helmholz equation as [8, 21]

$$\left\{\frac{\partial^2}{\partial x^2} + \frac{\partial^2}{\partial z^2} + \omega^2\mu\varepsilon\right\} H_y = 0. \tag{1}$$

E_x and E_z can be expressed in terms of H_y as [25] $E_x = -\frac{1}{j\omega\varepsilon}\frac{\partial H_y}{\partial z}$, $E_z = \frac{1}{j\omega\varepsilon}\frac{\partial H_y}{\partial x}$.

The fields H_y and E_z are continuous at $x = s$, and the field $E_z = 0$ at $x = 0$. Hence the boundary conditions are given by [8] at $x = 0$

$$\frac{\partial H_{ys}}{\partial x} = 0, \tag{2}$$

at $x = s$

$$\begin{cases} H_{ys} = H_{ya} \\ \frac{1}{\varepsilon}\frac{\partial}{\partial x}H_{ys} = \frac{1}{\varepsilon_0}\frac{\partial}{\partial x}H_{ya}. \end{cases} \tag{3}$$

H_{ys} and H_{ya} are the fields in the substrate and free space, respectively.

The fields are governed by the differential equations for E_x and E_z together with boundary conditions. In addition, H_{ya} should satisfy

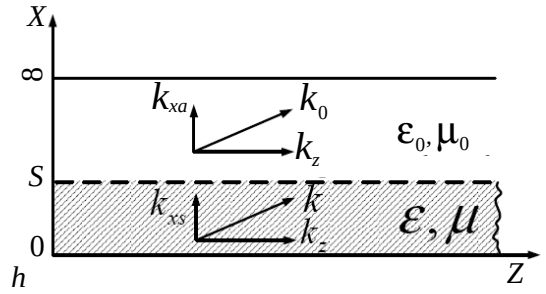

Figure 2. Wave number supportable by planer LHMs.

the radiation condition at $x = \infty$. The dielectric film is assumed to be sufficiently thin that only the first few modes of the guided modes are supported [26]. Then, the fields are expressed in detail as [8]

$$\begin{cases} H_{ya} = N_g a_g e^{-jk_{xa}(x-s)} e^{-jk_z z} \quad (x > s) \\ H_{ys} = N_g a_g \frac{\cos(k_{xs}x)}{\cos(k_{xs}s)} e^{-jk_z z} \quad (0 < x < s), \end{cases} \tag{4}$$

where

$$\begin{cases} k_{xa}^2 + k_z^2 = \omega^2 \mu_0 \varepsilon_0 \quad (x > s) \\ k_{xs}^2 + k_z^2 = \omega^2 \mu \varepsilon \quad (0 < x < s). \end{cases} \tag{5}$$

k_{xa}, k_{xs}, and k_z are complex transverse wave numbers as shown in Figure 2.

$$\begin{cases} k_{xa} = k'_{xa} + jk''_{xa} = \beta_{xa} - j\alpha_{xa}, \\ k_{xs} = k'_{xs} + jk''_{xs} = \beta_{xs} - j\alpha_{xs}, \\ k_z = k'_z + jk''_z = \beta_z - j\alpha_z, \end{cases} \tag{6}$$

where β and α are the phase constant and the attenuation constant, respectively. The partial differential of the magnetic fields in the two different regions are derived as

$$\begin{cases} \frac{\partial}{\partial x} H_{ys} = -N_g a_g k_{xs} tan(k_{xs} s) e^{-jk_z z} \\ \frac{\partial}{\partial x} H_{ya} = -jN_g a_g k_{xa} e^{-jk_z z}. \end{cases} \tag{7}$$

Based on the boundary condition Eqs. (2) and (3), the solutions satisfy the dispersion relation

$$k_{xs} \tan(k_{xs} s) = \varepsilon_r j k_{xa}, \tag{8}$$

where $\varepsilon_r = \varepsilon/\varepsilon_0$ is the relative permittivity of the material.

3. DISPERSION CHARACTERISTIC ANALYSIS

Dispersion relation of (8) is numerically estimated on the fundamental TM mode supported by the lossless film with permittivity $\varepsilon = \varepsilon_r \varepsilon_0$

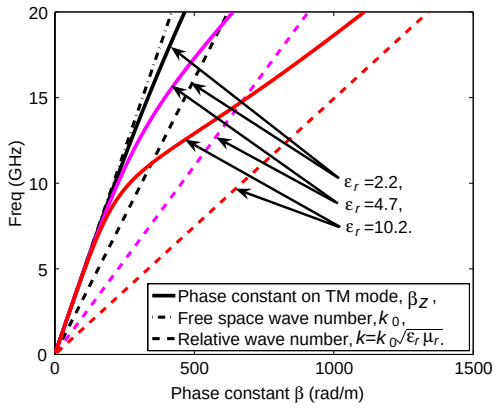

Figure 3. Dispersion relation on TM mode for the pure right-handed material.

and permeability $\mu = \mu_r\mu_0$ covered by the free space (ε_0, μ_0). The dispersion diagrams for the right-handed material with different permittivities have been calculated for reference. Then, the dispersion characteristics for the LH material and CRLH material are compared.

3.1. Right-handed Material

Figure 3 shows the dispersion characteristic supported by the conventional right-handed material with different permittivities (ε_r = 2.2, 4.7, 10.2) and permeability $\mu_r = 1$ based on the fundamental TM mode. The attenuation constant α_z is zero while the phase constant β_z follows $k_0 < \beta_z < k_0\sqrt{\varepsilon_r\mu_r}$. Based on the relation of Eq. (5), the complex wave number k_z in the substrate satisfies:

$$\omega^2\mu_0\varepsilon_0 < k_z^2 < \omega^2\mu\varepsilon \tag{9}$$

This condition makes

$$\begin{cases} k_{xa}^2 = \omega^2\mu_0\varepsilon_0 - k_z^2 < 0 \\ k_{xs}^2 = \omega^2\mu\varepsilon - k_z^2 > 0 \end{cases} \tag{10}$$

And then,

$$\begin{cases} \beta_{xa} = 0, \alpha_{xa} > 0 \\ \beta_{xs} > 0, \alpha_{xa} = 0 \end{cases} \tag{11}$$

The fields supported by the right-handed film are expressed as

$$\begin{cases} H_{ya} = N_g a_g e^{\alpha_{xa}(x-s)} e^{-j\beta_z z} & (x > s) \\ H_{ys} = N_g a_g \frac{\cos(\beta_{xs}x)}{\cos(\beta_{xs}s)} e^{-j\beta_z z} & (0 < x < s), \end{cases} \tag{12}$$

This means the field exponentially decays away from the surface at $x = s$, and propagates along the z-axis of the structure. It is a surface wave [27], Chapter 11.

3.2. Left-handed Material

Although no pure left-handed material (LHM) is found in nature until now, artificial LH structures [1, 3, 28, 29] and CRLH TL [7, 8, 12, 30] have been designed and investigated by a majority of groups. In the LH structure, both the effective permittivity and permeability of the material are realized as negative value. It is necessary to investigate the dispersion characteristics of the LHM. For simplicity and without loss of generality, the analyzed structure is the same as the right-handed case as shown in Figure 1 except $\varepsilon < 0$ and $\mu < 0$. From Maxwell's equations and boundary conditions (2) and (3), the magnetic field is derived as (4) and the complex wave number also satisfy the conditions as shown in (5), (6) and (8).

However, in some frequency, $\omega^2\mu_0\varepsilon_0 > \omega^2\mu\varepsilon$, and we cannot make $k_{xa}^2 = \omega^2\mu_0\varepsilon_0 - k_z^2 < 0$ and $k_{xs}^2 = \omega^2\mu\varepsilon - k_z^2 > 0$ either. If k_z^2 is a pure real number, then k_z can be a pure real number or imag number. The same applies to k_{xa}^2 and k_{xs}^2. If k_z is a pure real number (propagating), because $\omega^2\mu_0\varepsilon_0 > \omega^2\mu\varepsilon_{s0}$, then jk_{xa} and k_{xs} cannot be a pure real number (matching to the boundary condition) simultaneously. If the value of k_z is a pure imag number which means the waveguide works in stop band, because $\omega^2\mu_0\varepsilon_0 > \omega^2\mu\varepsilon$, then k_{xa} should be a pure real number, which is not possible. So that, k_z^2 should be a complex number. And the same as k_{xa}^2 and k_{xs}^2.

We again assume $k_{xa}^2 + k_z^2 = \omega^2\mu_0\varepsilon_0$ and $k_{xs}^2 + k_z^2 = \omega^2\mu\varepsilon$. k_{xa}, k_{xs}, and k_z are complex number as shown in Figure 4.

$$\begin{cases} k_{xa} = k'_{xa} + jk''_{xa} = \beta_{xa} - j\alpha_{xa} \\ k_{xs} = k'_{xs} + jk''_{xs} = \beta_{xs} - j\alpha_{xs} \\ k_z \ = k'_z + jk''_z = \beta_z - j\alpha_z \end{cases} \tag{13}$$

where $*'$ is the phase constant and $*''$ is the attenuation constant. In the substrate, when both k_z and k_{xs} are real, H_{ys} describes the field of a homogeneous plane wave. When at least one of the wave numbers ceases to be real, H_{ys} becomes an inhomogeneous plane wave.

For a homogeneous plane wave, we can define a real wave

$$k = k_{xs}\widehat{x} + k_z\widehat{z} \tag{14}$$

Introducing the radius vector: $r = x\widehat{x} + z\widehat{z}$, the constant phase planes in H_{ys} are given by $k \cdot r = contant$, which indicates that the plane wave is traveling in the direction of the phase front normal k. if k forms an

angle with the positive x axis, the phase velocity of the plane wave in the z-direction is fast in all directions but k.

For an inhomogeneous plane wave, it is obtained as shown in Figure 5,

$$\begin{cases} (k'_{xa} + jk''_{xa})^2 + (k'_z + jk''_z)^2 = \omega^2\mu_0\varepsilon_0 \\ (k'_{xs} + jk''_{xs})^2 + (k'_z + jk''_z)^2 = \omega^2\mu\varepsilon \end{cases} \tag{15}$$

$$\begin{cases} (k'^2_{xa} + k'^2_z) - (k''^2_{xa} + k''^2_z) = \omega^2\mu_0\varepsilon_0 \\ (k'^2_{xs} + k'^2_z) - (k''^2_{xs} + k''^2_z) = \omega^2\mu\varepsilon_{s0} \end{cases} \tag{16}$$

and $k'_z k''_z + k'_{xa} k''_{xa} = 0$ and $k'_z k''_z + k'_{xs} k''_{xs} = 0$

For an inhomogeneous plane wave, it is got:

$$\begin{cases} \beta_a = k'_{xa}\widehat{x} + k'_z\widehat{z} \quad \alpha_a = -(k''_{xa}\widehat{x} + k''_z\widehat{z}) \\ \beta_s = k'_{xs}\widehat{x} + k'_z\widehat{z} \quad \alpha_s = -(k''_{xs}\widehat{x} + k''_z\widehat{z}) \end{cases} \tag{17}$$

Then, the over questions are rewritten as:

$$\begin{cases} \beta_a^2 - \alpha_a^2 = \omega^2\mu_0\varepsilon_0 \quad \beta_s^2 - \alpha_s^2 = \omega^2\mu\varepsilon \\ \beta_a\alpha_a = 0 \quad \beta_s\alpha_s = 0 \end{cases} \tag{18}$$

Introducing the radius vector for the inhomogeneous plane wave: $\widehat{r} = x\widehat{x} + z\widehat{z}$. And then, the solutions for the differential equations is:

$$\begin{aligned} H_{ya} &= N_g a_g e^{-jk_{xa}(x-s)} e^{-jk_z z} = N_g a_g e^{-j(k'_{xa}+jk''_{xa})(x-s)} e^{-j(k'_z+jk''_z)z} \\ &= N_g a_g e^{-j(k'_{xa}+jk''_{xa})s} e^{-j(k'_{xa}\widehat{x}+k'_z\widehat{z})} e^{(k''_{xa}\widehat{x}+k''_z\widehat{z})} \\ &= N_g a_g e^{jk_{xa}s} e^{-j(\beta_a-\alpha_a)\widehat{r}} \end{aligned} \tag{19}$$

$$\begin{aligned} H_{ys} &= N_g a_g \frac{\cos(k_{xs}x)}{\cos(k_{xs}s)} e^{-jk_z z} = N_g a_g \frac{\cos((k'_{xs}+jk''_{xs})x)}{\cos(k_{xs}s)} e^{-j(k'_z+jk''_z)z} \\ &= \frac{N_g a_g}{\cos(k_{xs}s)} \frac{e^{j(k'_{xs}+jk''_{xs})x} + e^{-j(k'_{xs}+jk''_{xs})x}}{2} e^{-j(k'_z+jk''_z)z} \\ &= \frac{N_g a_g}{2\cos(k_{xs}s)} \left(e^{-j(\beta_s^*-j\alpha_s^*)r_s^*} + e^{-j(\beta_s-j\alpha_s)r_s} \right) \end{aligned} \tag{20}$$

where α_a and α_s points in the direction of the most rapid amplitude decrease, β_a and β_s gives the direction of propagation and that of the power flow of the wave.

- In the substrate, the wave is shown as in (20). In z-direction, the wave equation is $H_{y0sz} = e^{-j(k'_z+jk''_z)z}$, which means the wave propagates with loss. k'_z is the phase constant, and $-k''_z$ is the attenuation constant. In x-direction, the wave is shown as $H_{y0sx} = \cos((k'_{xs} + jk''_{xs})x)$. This shows the wave is a pair of composite wave including two conjugate symmetry waves as shown in Figure 4. This waves is liking a standing wave, but it is lossy.

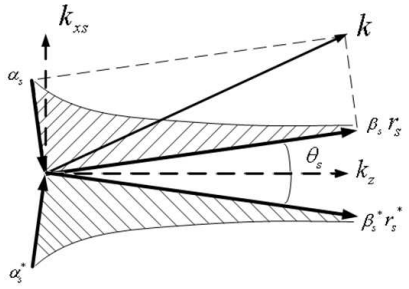

Figure 4. Inhomogeneous plane TM wave in LHM in substrate.

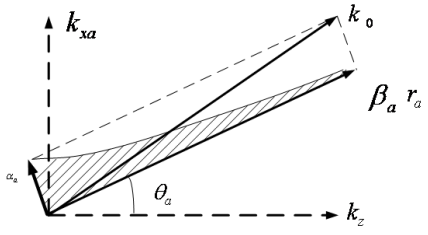

Figure 5. An inhomogeneous plane TM wave in LHM in freespace.

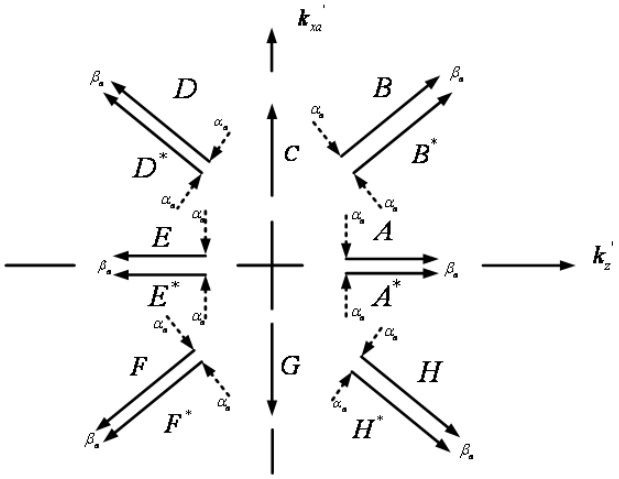

Figure 6. The wave types of inhomogeneous plane TM waves in LHM.

- In the free-space, a guided-wave field attenuates along z and leaky-wave increases exponentially away from the $x = 0$ plane. $\beta_a^2 - \alpha_a^2 = \omega^2\mu\varepsilon$ implies $|\beta_a| = \sqrt{\omega^2\mu\varepsilon}\sqrt{1 + \frac{{\alpha_a}^2}{\omega^2\mu\varepsilon}}$ which states that the inhomogeneous plane wave is always a slow wave in its direction of propagation as shown in Figure 5. However, the projection β_{az} of β_a on the z direction may correspond to either a fast or a slow wave. In the freespace, there are some cases as shown in Figure 6.
  A: represent a proper surface wave, which for TM polarization can propagate on an inductive modal ($X > 0$) impedance.

A*: noncontributing. improper surface wave.
B: represent a complex wave which radiates out of the surface but decays away from it. This wave (or rather its counterpart, $-kz$) is of importance in backward wave radiation from periodic structure and is utilized in log-periodic antennas.
B*: leaky wave. Forward-fire, (reprensents waves that violate the radiation condition at $x\infty$. for TM polarization such waves arise when X is capacitive, as required by $\alpha_a < 0$.)
D: LHMs, represent a complex wave which radiates out of the surface but decays away from it.
D*: LHMs, leaky-wave, back-fire.
E: LHMs, proper surface wave.
E*: LHMs, noncontributing. improper surface wave.
F: LHMs, lossy surface wave.
F*: LHMs, noncontributing.
H: lossy surface wave. Here β_a, and therefore the power flow, has a component into the surface, as required, to cover the losses.
H*: noncontributing.
A*, B*, D*, E*, F*, H* represent waves that violate the radiation condition at $x\infty$. for TM polarization such waves arise when X is capacitive, as required by $\alpha_a < 0$. H* and A*, F* and E*: do not contribute directly to the aperture field. However, they may be of some importance for the case of end-fire radiation in that their presence may require a modification of the steepest-descent procedure. This shows that the wave radiate from forward direction to backward direction.

Based on the analysis for conventional RHMs [19], the transverse resonance relation based on Figure 7 reads

$$Z(k_z, k_0) + \frac{k_{xa}}{\omega\varepsilon_0} = 0 \tag{21}$$

where $Z(k_z, k_0) = R - jX$, and $k_z = \beta_z - j\alpha_z$, $k_{xa} = \beta_a - j\alpha_a$. And then, we get as shown in Figure 7.

$$\frac{\beta_a - j\alpha_a}{\omega\varepsilon_0} = -R + jX \tag{22}$$

For $x > 0$, any TM guided wave supportable by the structure has this relationship. Consequently, the various guided wave types correspond to the possible classes of plane waves which may exist in free space above the interface. These plane waves are characterized by the various combinations of k_z and k_{xa}, which in turn are determined from in accordance with the signs of R and X.

$$\begin{aligned} signX &= -sign\alpha_a \\ -signR &= sign\beta_a \end{aligned} \tag{23}$$

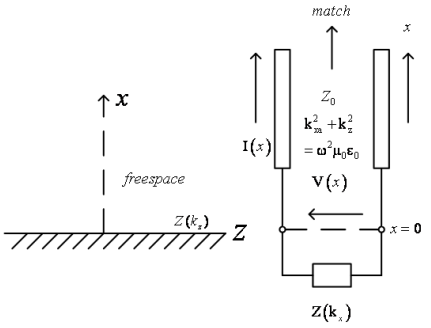

Figure 7. Geometry of the guiding plane interface and transverse equivalent network for TM modes [19].

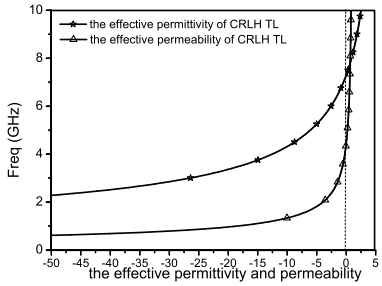

Figure 8. Effective permittivity and permeability and their dispersion behaviour.

3.3. Numerical Results of the Problem

Figure 8 shows the effective permittivity (ε) and permeability (μ) of the material, which can be given by $\varepsilon = \varepsilon_0\varepsilon_r - \frac{1}{\omega^2 L\Lambda}$, and $\mu = \mu_0 - \frac{1}{\omega^2 C\Lambda}$ [6].

Based on the dispersion relation as predicted by (8), Figure 9 shows that in the LH passband region, $f_A \sim f_C$, both the permittivity and the permeability are negative. In the stopband region ($f_C \sim f_E$), $\mu > 0$ and $\varepsilon < 0$, which is demonstrated to be an epsilon-negative (ENG) medium. In the RH passband region($f_E \sim 9.5\,\text{GHz}$), $\mu > 0$, $\varepsilon > 0$, the medium will be designated a double positive (DPS) medium.

For the dispersion relation (8), the lowest cutoff (Bragg) frequency f_0 associated with this dispersion curve is also determined from the condition $\beta d = \pi$, as shown in Figure 9. Setting $\beta = 0$ in (8), the solutions of the dispersion equation in frequency yield the desired cutoff frequencies f_C and f_E as shown in Figure 9. With the affection of $k_i \neq 0$, the upper cutoff frequencies are the same for both $k_i \neq 0$ and $k_i = 0$ ($f_E = f'_E$). But for $k_i \neq 0$, the lower cutoff frequency is lower than that when $k_i = 0$ ($f_C = f'_D$), which also give that the bandwidth of the stopband is wider than that when $k_i = 0$. And in the passband, for lower and higher frequency, the phase constants approach that for $k_i = 0$, but it will not cross the curve. In the stopband ($f_C \sim f_E$), the propagation constant is complex. As shown in Figure 9, the phase constant is equal to that in the air ($\beta^2 = \omega^2\mu_0\varepsilon_0$), and then passes to $\beta\Lambda = \pi$ at $f = f_{Bragg}$. there is a stopband because of the effect of surface ware in the lower frequency and Bragg reflection in higher frequency. The curve between f_B and f_C, f_E and f_G show leaky wave regions inside of cure of $\beta^2 = \omega^2\mu_0\varepsilon_0$ and the region between f_B and f_C has been used for left handed leaky wave antenna design.

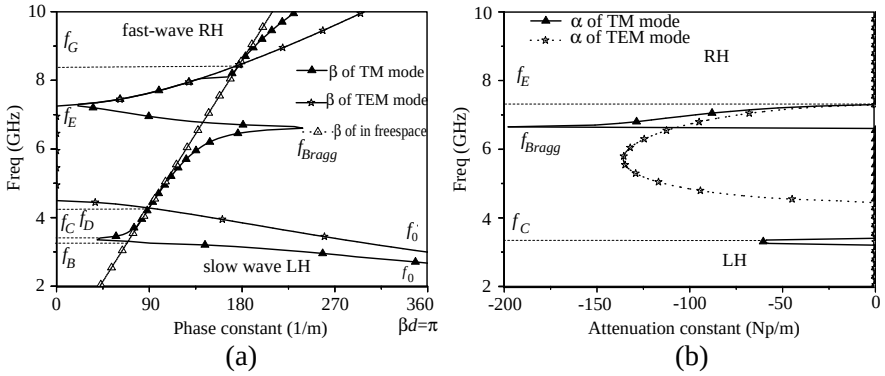

Figure 9. Propagation constant of left handed TM mode waveguide, unbalanced case.

4. CONCLUSION

We have proposed and introduced a technique for the analysis of the LHMs. The dispersion properties are rigorously derived from Maxwell's equation for both right-handed material and composite right/left handed material. In a lossless guiding structure with right-handed material, it is noted the structure represents simple waves that propagate without attenuation ($\beta \neq 0$ and $\alpha = 0$) or decay exponentially without phase variation ($\beta = 0$ and $\alpha \neq 0$). However, in a lossless guiding structure with composite right/left handed material, the electromagnetic waves become inhomogeneous plane waves since the wave numbers ceases to be real and become complex numbers. Through introducing a radius vector, phase and attenuation constants are rewritten as real number for the inhomogeneous plane wave following the direction of the propagation of the plane wave front. The fundamental properties of bound, surface and leaky modes of metamaterial based grounded dielectric waveguide have been analyzed. Typical backward wave characteristic of volume and surface wave modes are found from the distribution of Poynting power to the transverse direction of waveguide for the lossless guiding structure with composite right/left handed material.

REFERENCES

1. Veselago, V. G., "Electrodynamics of substances with simultaneously negative values of sigma and mu," *Soviet Physics Uspekhi-Ussr*, Vol. 10, 509, 1968.

2. Pendry, J. B., A. J. Holden, W. J. Stewart, and I. Youngs, "Extremely low frequency plasmons in metallic mesostructures," *Phys. Rev. Lett.*, Vol. 76, 4773–4776, 1996.
3. Pendry, J. B., A. J. Holden, D. J. Robbins, and W. J. Stewart, "Magnetism from conductors and enhanced nonlinear phenomena," *IEEE Trans. Microw. Theory Tech.*, Vol. 47, 2075–2084, 1999.
4. Smith, D. R., W. J. Padilla, D. C. Vier, S. C. Nemat-Nasser, and S. Schultz, "Composite medium with simultaneously negative permeability and permittivity," *Phys. Rev. Lett.*, Vol. 84, 4184–4187, 2000.
5. Shelby, R. A., D. R. Smith, and S. Schultz, "Experimental verification of a negative index of refraction," *Science*, Vol. 292, 77–79, 2001.
6. Eleftheriades, G. V., A. K. Iyer, and P. C. Kremer, "Planar negative refractive index media using periodically L-C loaded transmission lines," *IEEE Trans. Microw. Theory Tech.*, Vol. 50, 2702–2712, 2002.
7. Caloz, C. and T. Itoh, "Transmission line approach of left-handed (LH) materials and microstrip implementation of an artificial LH transmission line," *IEEE Trans. Antennas Propagat.*, Vol. 52, 1159–1166, 2004.
8. Tsutsumi, M., C. Jin, and A. Alphones, "Leaky wave phenomenon from double periodic left handed waveguide," *Asia-Pacific Microwave Conf.*, 1238–1241, Singapore, 2009.
9. Jin, C., A. Alphones, and M. Tsutsumi, "Leaky-wave characteristics from double periodic composite right/left handed transmission lines," *IET Proc. Microwave Antennas Propag.*, Vol. 5, No. 12, 1399–1407, 2011.
10. Jin, C., A. Alphones, and M. Tsutsumi, "Double periodic composite right/left handed transmission line and its applications to compact leaky-wave antennas," *IEEE Trans. Antennas Propagat.*, Vol. 59, No. 10, 3679–3686, 2011.
11. Jin, C. and A. Alphones, "Leaky-wave radiation behavior from a double periodic composite right/left handed substrate integrated waveguide," *IEEE Trans. Antennas Propagat.*, Vol. 60, No. 4, 1727–1735, 2012.
12. Caloz, C. and T. Itoh, *Electromagnetic Metamaterials Transmission Line Theory and Microwave Applications,* Wiley, New York, 2006.
13. Yu, F. Y. A. and A. Z. Elsherbeni, "A dual band circularly

polarized ring antenna based on composite right and left handed metamaterials," *Progress In Electromagnetics Research*, Vol. 78, 73–81, 2008.

14. Jin, C., A. Alphones, and L. C. Ong, "Broadband leaky-wave antenna based on composite right/left handed substrate integrated waveguide," *Electron. Lett.*, Vol. 46, No. 24, 1584–1585, 2010.
15. Zhou, X. Z. B., H. Li, and T.-J. Cui, "Broadband and high-gain planar vivaldi antennas based on inhomogeneous anisotropic zeroindex metamaterials," *Progress In Electromagnetics Research*, Vol. 120, 235–247, 2011.
16. Huang, J.-Q. and Q.-X. Chu, "Compact UWB band-pass filter utilizing modified composite right/left-handed structure with cross coupling," *Progress In Electromagnetics Research*, Vol. 107, 179–186, 2010.
17. Garcia-Perez, D. S.-V. O., L. E. Garcia-Munoz, and V. Gonzalez-Posadas, "Multiple order dual-band active ring filters with composite right/left-handed cells," *Progress In Electromagnetics Research*, Vol. 104, 201–219, 2010.
18. Jin, C. and A. lphones, "Compact interdigital microstrip band pass filter," *Microwave Opt. Technol. Lett.*, Vol. 52, 2128–2132, 2010.
19. Collin, R. E. and F. J. Zucker, *Antenna Theory,* 2nd edition, McGraw-Hill, New York, London, 1969.
20. Seshadri, S. R., "Search results coupling of guided modes in thin films with surface corrugation," *J. of Appl. Phys.*, Vol. 63, R115–R146, 1988.
21. Alphones, A. and M. Tsutsumi, "Leaky-wave radiation from a periodically photoexcited semiconductor slab waveguide," *IEEE Trans. Microw. Theory Tech.*, Vol. 43, 2435–2441, 1995.
22. Yakovlev, A. B., M. G. Silveirinha, O. Luukkonen, C. R. Simovski, I. S. Nefedov, and S. A. Tretyakov, "Characterization of surfacewave and leaky-wave propagation on wire-medium slabs and mushroom structures based on local and nonlocal homogenization models," *IEEE Trans. Microw. Theory Tech.*, Vol. 57, 2700–2714, 2009.
23. Aznar, F., M. Gil, J. Bonache, and F. Martin, "Revising the equivalent circuit models of resonant-type metamaterial transmission lines," *IEEE MTTS International Microwave Symposium Digest*, 322–325, Atlanta, GA, 2008.
24. Cassivi, Y., L. Perregrini, P. Arcioni, M. Bressan, K. Wu, and G. Conciauro, "Dispersion characteristics of substrate integrated

rectangular waveguide," *IEEE Microw. and Wireless Compon. Lett.*, Vol. 12, 333–335, 2002.

25. Pozar, D. M., *Microwave Engineering,* 3rd Edition, Wiley, New York, 2004.
26. Kasraian, M., "Double-grating thin-film devices based on secondorder Bragg interaction," *J. of Appl. Phys.*, Vol. 75, 7639–7652, 1994.
27. Collin, R. E., *Field Theory of Guided Waves*, IEEE Press, New York, 1990.
28. Smith, D. R., D. C. Vier, N. Kroll, and S. Schultz, "Direct calculation of permeability and permittivity for a left-handed metamaterial," *Appl. Phys. Lett.*, Vol. 77, No. 14, 2246–2248, 2000.
29. Ziolkowski, R. W. and E. Heyman, "Wave propagation in media having negative permittivity and permeability," *Phys. Rev. E*, Vol. 64, 056625, 2001.
30. Iyer, A. K. and G. V. Eleftheriades, "Negative refractive index metamaterials supporting 2-D waves," *IEEE MTT-S International Microwave Symposium Digest*, 1067–1070, Hamilton, R., Ed., 2002.